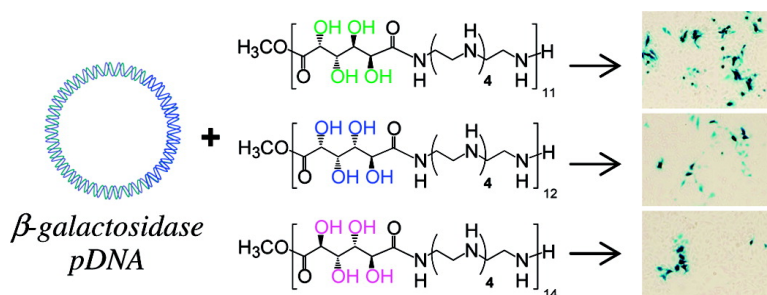


Hydroxyl Stereochemistry and Amine Number within Poly(glycoamidoamine)s Affect Intracellular DNA Delivery

Yemin Liu, and Theresa M. Reineke

J. Am. Chem. Soc., **2005**, 127 (9), 3004-3015 • DOI: 10.1021/ja0436446 • Publication Date (Web): 11 February 2005

Downloaded from <http://pubs.acs.org> on March 24, 2009



More About This Article

Additional resources and features associated with this article are available within the HTML version:

- Supporting Information
- Links to the 12 articles that cite this article, as of the time of this article download
- Access to high resolution figures
- Links to articles and content related to this article
- Copyright permission to reproduce figures and/or text from this article

[View the Full Text HTML](#)



Hydroxyl Stereochemistry and Amine Number within Poly(glycoamidoamine)s Affect Intracellular DNA Delivery

Yemin Liu and Theresa M. Reineke*

Contribution from the Department of Chemistry, University of Cincinnati,
Cincinnati, Ohio 45221-0172

Received October 19, 2004; E-mail: Theresa.Reineke@uc.edu

Abstract: Nucleic acid drugs have great potential to treat many devastating ailments, but their application has been hindered by the lack of efficacious and nontoxic delivery vehicles. Here, a new library of poly(glycoamidoamine)s (**D1–D4**, **G1–G4**, and **M1–M4**) has been synthesized by polycondensation of esterified D-glucaric acid (**D**), dimethyl-*meso*-galactarate (**G**), and D-mannaro-1,4:6,3-dilactone (**M**) with diethylene-triamine (**1**), triethylenetetramine (**2**), tetraethylenepentamine (**3**), and pentaethylenhexamine (**4**). The stereochemistry of the carbohydrate hydroxyl groups and the number of amine units have been systematically changed in an effort to examine how the polymer chemistry affects the plasmid DNA (pDNA) binding affinity, the compaction of pDNA into nanoparticles (polyplexes), the material cytotoxicity, and the efficacy of nucleic acid delivery. The polymers with four secondary amines (**D4**, **G4**, and **M4**) between the carbohydrates were found to have the highest pDNA binding affinity and the galactarate polymers generally yielded the smallest polyplexes. Delivery studies with pDNA containing the firefly luciferase or β -galactosidase reporter genes in BHK-21, HeLa, and HepG2 cells demonstrated that all of the poly(glycoamidoamine)s deliver pDNA without cytotoxicity. Polymers **D4**, **G4**, and **M4** displayed the highest delivery efficiency, where **G4** was found to be a particularly effective delivery vehicle. Heparin competition assays indicated that this may be a result of the higher pDNA binding affinity displayed by **G4** as compared to **D4** and **M4**. Polyplexes formed by polymers with weaker pDNA affinities may dissociate at the cell surface due to interactions with negatively charged glycosaminoglycans, which would cause a decrease in the number of polyplexes that are endocytosed.

Introduction

The completion of the human genome project will herald revolutionary advances in modern medicine through the development of nucleic acid-based treatments.¹ DNA, RNA, and PNA (peptide nucleic acids) have great potential to become novel therapeutics in the emerging areas of RNA interference,² gene-based therapy,^{3–5} genetic vaccines,⁶ and oligonucleotide drugs.⁷ However, the utility of these forthcoming techniques is completely dependent on the success of nucleic acid delivery to the specific site of disease. The development of vehicles that carry genetic materials into cells in a manner that is efficient, nontoxic, and does not interfere with normal cellular functions has become

the most fundamental and difficult problem facing the advancement of these technologies.^{8–12} To this end, both virus-mediated^{5,13–15} and nonviral systems^{8,9,12,16–18} are currently being investigated as modalities for nucleic acid transfer.

Viruses are naturally evolved delivery vehicles; they possess features that trigger efficient cellular uptake via the endocytotic pathway, facilitate the release of foreign genetic material into the cytoplasm, and direct the transport into the nucleus.³ Genetically modified viruses have been extensively utilized in gene therapy clinical trials owing to the efficient mechanisms they possess to circumvent all of these biological barriers during

- (1) (a) The International Human Genome Sequencing Consortium. *Nature* **2001**, *409*, 928–933. (b) The International Human Genome Sequencing Consortium. *Nature* **2001**, *409*, 934–941. (c) Bell, J. *Nature* **2004**, *429*, 453–456. (d) Tishkoff, S. A.; Verelli, B. C. *Curr. Opin. Genet. Dev.* **2003**, *13*, 569–575. (e) Langer, R.; Tirrell, D. A. *Nature* **2004**, *428*, 487–492.
- (2) (a) Scherer, L. J.; Rossi, J. J. *Nat. Biotech.* **2003**, *21*, 1457–1465. (b) Scherr, M.; Morgan, M. A.; Eder, M. *Curr. Med. Chem.* **2003**, *10*, 245–256. (c) Medema, R. H. *Biochem. J.* **2004**, *380*, 593–603.
- (3) Kaneda, Y. *Curr. Mol. Med.* **2001**, *1*, 493–499.
- (4) (a) Ledley, F. D. *Pharm. Res.* **1996**, *13*, 1595–1614. (b) Mahato, R. I.; Smith, L. C.; Rolland, A. P. *Adv. Genet.* **1999**, *41*, 95–156.
- (5) Rubanyi, G. M. *Mol. Aspects Med.* **2001**, *22*, 113–142.
- (6) (a) Lee, L. K.; Mount, C. N.; Shamlou, P. A. *Chem. Eng. Sci.* **2001**, *56*, 3163–3172. (b) Leitner, W. W.; Ying, H.; Restifo, N. P. *Vaccine* **1999**, *18*, 765–777.
- (7) (a) Neilsen, P. E. *Mol. Biotechnol.* **2004**, *26*, 233–248. (b) Tomita, N.; Azuma, H.; Kaneda, Y.; Ogiwara, T.; Morishita, R. *Curr. Drug Targets* **2003**, *4*, 339–346.

- (8) Davis, M. E. *Curr. Opin. Biotechnol.* **2002**, *13*, 128–131.
- (9) Luo, D.; Saltzman, W. M. *Nat. Biotechnol.* **2000**, *18*, 33–37.
- (10) Ma, H.; Diamond, S. L. *Curr. Pharm. Biotechnol.* **2001**, *2*, 1–17.
- (11) Hapala, I. *Crit. Rev. Biotechnol.* **1997**, *17*, 105–122.
- (12) Han, S.; Mahato, R. I.; Sung, Y. K.; Kim, S. W. *Mol. Ther.* **2000**, *2*, 302–317.
- (13) Zhu, J.; Grace, M.; Casale, J.; Chang, A. T. I.; Musco, M. L.; Bordens, R.; Greenberg, R.; Schaeffer, E.; Indelicato, S. R. *Hum. Gene Ther.* **1999**, *10*, 113–121.
- (14) (a) Lee, J. H.; Baker, T. J.; Zabner, J.; Bertozzi, C. R.; Wiemer, D. F.; Welsh, M. J. *J. Biol. Chem.* **1999**, *274*, 21878–21884. (b) Kass-Eisler, A.; Falck-Pedersen, E.; Alvira, M.; Rival, J.; Buttrick, P. M.; Wittenberg, B. A.; Cipriani, L.; Leinwand, L. A. *Proc. Natl. Acad. Sci. U.S.A.* **1993**, *90*, 11498–11502. (c) French, B. A.; Mazur, W.; Geske, R. S.; Bolli, R. *Circulation* **1994**, *90*, 2414–2424.
- (15) Smith, A. E. *Annu. Rev. Microbiol.* **1995**, *49*, 807–818.
- (16) De Smedt, S. C.; Demeester, J.; Hennink, W. E. *Pharm. Res.* **2000**, *17*, 113–126.
- (17) Davis, M. E.; Pun, S. H.; Bellocq, N. C.; Reineke, T. M.; Popielarski, S. R.; Mishra, S.; Heidel, J. D. *Curr. Med. Chem.* **2004**, *11*, 1241–1253.
- (18) Pannier, A. K.; Shea, L. D. *Mol. Ther.* **2004**, *10*, 19–26.

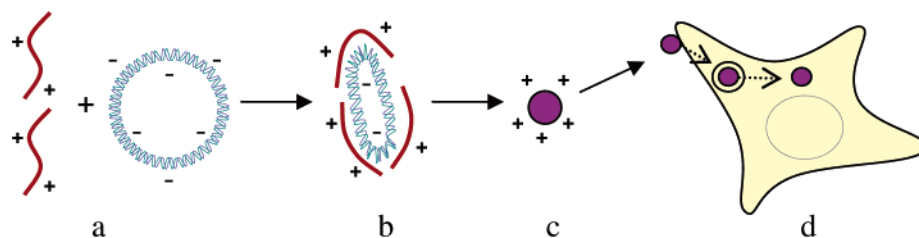


Figure 1. Scheme of polyplex formation and cellular uptake. (a) Polycations electrostatically associate with the anionic plasmid DNA (pDNA) phosphate backbone. (b) Polymer-pDNA binding and compaction. (c) Polyplex formation. (d) Cellular uptake through the endocytotic pathway and endosomal release.

the delivery process.^{3,5,13,15} Unfortunately, severe problems have occurred with viral vectors that have hindered their use. For example, viral carriers can induce immunogenicity, inflammation, and randomly integrate DNA into the genome *in vivo*.^{9,19} In addition, their finite size limits the amount of genetic material that can be incorporated within these carriers.^{12,15}

Both the advantages and disadvantages of viral delivery systems have inspired the design and investigation of synthetic materials that may retain the efficient biological mechanisms characteristic of viral delivery yet evade the devastating side effects *in vivo*. Ideal nonviral systems must be nontoxic, incorporate a large capacity of nucleic acids, prevent genetic material from enzymatic damage, be resistant to aggregation and premature nucleic acid release during transport, and still retain the ability to unpack the genetic material after efficient intracellular delivery.^{8,9,12,16,20,21} Indeed, the future promise of utilizing synthetic vectors to deliver genetic medicines lies in creative chemical synthesis in an effort to gain fundamental insight into the material characteristics that facilitate efficient, nontoxic, and stable transport of nucleic acid drugs into diseased cells.

Polymers are currently being studied as practical alternatives to viral systems because of their promise to avoid the difficulties previously mentioned. As shown in Figure 1, polycations have the ability to form electrostatic complexes with and compact DNA into small viral-like nanostructures termed polyplexes (polymer + DNA complexes).^{17,22,23} Polyplexes can be uptaken into cells through endocytosis and deliver genetic material that can either bind a specific gene and down regulate expression (antisense agents), be integrated into the genome, or exist exogenously where the gene is transcribed and translated.²⁴ However, polymers commonly have low delivery efficiency and/or high cytotoxic profiles.^{8–10,21} Also, subtle differences in the polymer chemical and structural properties such as molecular weight,²⁵ hydrophobicity,¹⁷ charge density,²² and charge type,²³ can significantly affect all of the processes involved in the biological delivery of nucleic acids. Polyethylenimine (PEI) and chitosan (Figure 2), two well-studied gene delivery vectors, are

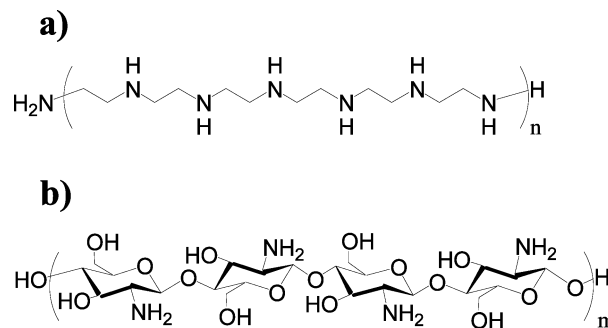


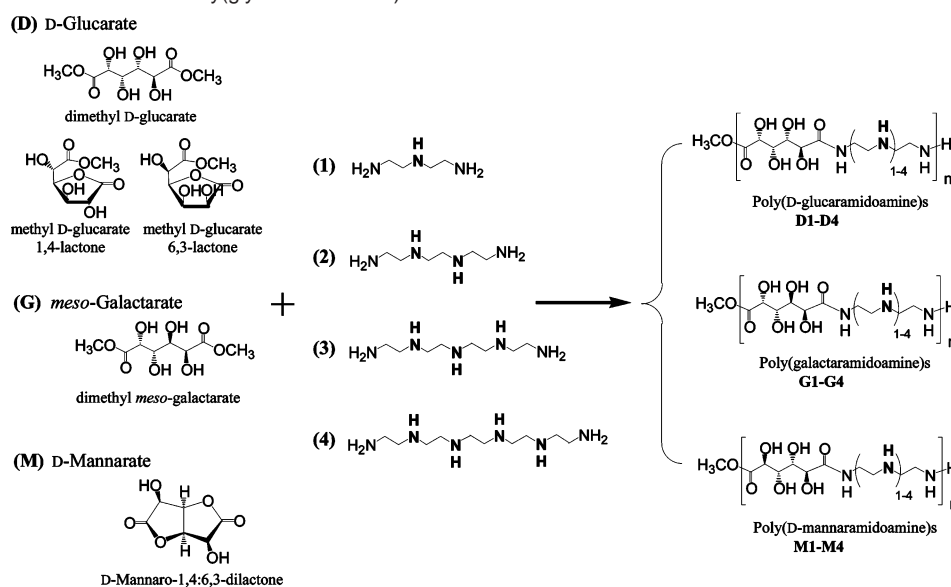
Figure 2. Structures of two commonly studied polymeric vectors: (a) linear polyethylenimine (L-PEI) and (b) chitosan.

such examples. PEI is generally accepted as one of the most efficient polymeric delivery vehicles. The high density of secondary amines allows effective nucleic acid binding and compaction.^{26,27} Larger molecular weight versions of this polymer (i.e. 25 kDa) display effective intracellular gene delivery with almost all cell lines.^{25,28} Unfortunately, the most efficacious molecular weight ranges exhibit high cytotoxicity in most cases, which has inhibited its clinical development.^{22,29} Conversely, chitosan, a polysaccharide containing primary amine groups (derived from deacetylated chitin), is nontoxic at high concentrations and at all molecular weight ranges.^{30,31} Although it shows effective nucleic acid binding and compaction, the delivery efficiency exhibited by this vector is quite low in most cell lines.^{22,31,32}

Inspired by the chemical structures and biological properties of both PEI and chitosan, we have polymerized D-glucarate, *meso*-galactarate, and D-mannarate comonomers with a series of di-primary amines that contain between 1 and 4 secondary amine units. A library of structures (Scheme 1) that incorporate the promising characteristics of PEI and chitosan (secondary amines and saccharide groups) have been created. Previously, we reported with the series of poly(D-glucaramidoamine)s, as the number of secondary amines between the D-glucarate repeat units increased, gene expression was enhanced in BHK-21

- (19) (a) Fox, J. L. *Nat. Biotechnol.* **2003**, *21*, 217. (b) Marshall, E. *Science* **1999**, *286*, 2244–2245.
 (20) Cristiano, R. J.; Curiel, D. T. *Cancer Gene Ther.* **1996**, *3*, 49–57.
 (21) Li, S.; Ma, Z. *Curr. Gene Ther.* **2001**, *1*, 201–226.
 (22) Liu, Y.; Wenning, L.; Lynch, M.; Reineke, T. M. *J. Am. Chem. Soc.* **2004**, *126*, 7422–7423.
 (23) (a) Reineke, T. M.; Davis, M. E. *Bioconjugate Chem.* **2003**, *14*, 247–254. (b) Reineke, T. M.; Davis, M. E. *Bioconjugate Chem.* **2003**, *14*, 255–261.
 (24) (a) Bieber, T.; Meissner, W.; Kostin, S.; Niemann, A.; Elsasser, H. P. *J. Controlled Release* **2002**, *82*, 441–454. (b) Felgner, J. H.; Kumar, R.; Sridhar, C. N.; Wheeler, C. J.; Tsai, Y. J.; Border, R.; Ramsey, P.; Martin, M.; Felgner, P. L. *J. Biol. Chem.* **1994**, *269*, 2550–2561. (c) Godbey, W. T.; Wu, K. K.; Mikos, A. G. *Proc. Natl. Acad. Sci. U.S.A.* **1999**, *96*, 5177–5181. (d) Kabanov, A. V.; Lemieu, P.; Vinogradov, S.; Alakhov, V. *Adv. Drug Delivery Rev.* **2002**, *54*, 223–233.
 (25) Godbey, W. T.; Wu, K. K.; Mikos, A. G. *J. Biomed. Mater. Res.* **1999**, *45*, 268–275.

- (26) von Harpe, A.; Petersen, H.; Li, Y.; Kissel, T. *J. Controlled Release* **2000**, *69*, 309–322.
 (27) Choosakoonkriang, S.; Lobo, B. A.; Koe, G.; Koe, J. G.; Middaugh, C. R. *J. Pharm. Sci.* **2003**, *92*, 1710–1722.
 (28) Boussif, O.; Lezoualch, F.; Zanta, M. A.; Mergny, M. D.; Scherman, D.; Demeneix, B.; Behr, J. P. *Proc. Natl. Acad. Sci. U.S.A.* **1995**, *92*, 7297–7301.
 (29) (a) Fischer, D.; Bieber, T.; Li, Y.; Elsasser, H. P.; Kissel, T. *Pharm. Res.* **1999**, *16*, 1273–1279. (b) Chollet, P.; Favrot, M. C.; Hurbain, A.; Coll, J. L. *J. Gene Med.* **2002**, *4*, 84–91. (c) Godbey, W. T.; Mikos, A. G. *J. Controlled Release* **2001**, *72*, 115–125.
 (30) (a) Hoggard, M. K.; Tubulekas, I.; Guan, H.; Edwards, K.; Nilsson, M.; Varum, K. M.; Artursson, P. *Gene Ther.* **2001**, *8*, 1108–1121. (b) Liu, W. G.; Yao, K. D. *J. Controlled Release* **2002**, *83*, 1–11.
 (31) MacLaughlin, F. C.; Mumper, R. J.; Wang, J.; Tagliaferrri, J. M.; Gill, I.; Hinchliffe, M.; Rolland, A. P. *J. Controlled Release* **1998**, *56*, 259–272.
 (32) Erbacher, P.; Zou, S.; Bettinger, T.; Steffan, A. M.; Remy, J. S. *Pharm. Res.* **1998**, *15*, 1332–1339.

Scheme 1. Synthetic Scheme for the Poly(glycoamidoamine)s^a

^a Polymers are named according to the carbohydrate moieties and the number of secondary amines per repeat unit.

(Syrian golden hamster kidney) cells.²² In the present study, our scope was broadened to elucidate whether this is a general trend for additional synthetic poly(glycoamidoamine)s in multiple cell lines. Also, this study was performed to gain an understanding of how the hydroxyl stereochemistry in three different series of poly(glycoamidoamine)s affects their abilities to deliver genetic material.

Here, we reveal that polymers containing carbohydrate moieties along a PEI-like polymer backbone can retain the biocompatible properties of chitosan and in some cases the high delivery efficiency of PEI. In addition to the number of amines, the stereochemistry of the hydroxyl units within differing poly(glycoamidoamine)s is shown to have a significant effect on several biological properties. Gel electrophoretic shift assays reveal that the carbohydrate groups and the number of amines considerably influence the pDNA binding affinity of the synthetic polymers. Dynamic light scattering experiments also demonstrate that the hydroxyl stereochemistry and the amine stoichiometry play a role in the ability of these structures to compact pDNA into nanostructures. Furthermore, reporter gene delivery experiments with a variety of mammalian cells show that both the hydroxyl stereochemistry and the amine number clearly alter the ability of the genetic material to be delivered into cells, however, this effect is cell-type dependent. These studies represent our first-step toward understanding how specific chemical functionalities within polymers affect the ability of synthetic materials to deliver nucleic acids to living cells in a nontoxic manner. Studies of this type are important to the rational design and development of synthetic biomaterials and will serve as a basis for future exploration of the necessary chemical and structural features for functional genetic delivery systems.

Experimental Section

I. Synthesis and Purification of Monomers and Copolymers.

General. All reagents used in the synthesis, if not specified, were obtained from Aldrich Chemical Co. (Milwaukee, WI) with purity of more than 98%, and were used without further purification. Linear PEI (L-PEI, 25 kDa) was obtained from Avanti Polar Lipids (Alabaster,

AL) where it is sold under the name of Jet-PEI. Crude pentaethylenehexamine was purchased from Acros (Morris Plains, NJ), and was purified according to a reported procedure.^{22,33} The esterified D-glucaric acid comonomer was synthesized as previously described.^{22,34} The mass spectra were obtained from an IonSpec HiResESI mass spectrometer in positive ion mode. Melting points of polymers were measured with a Netzsch simultaneous TG-DTA/DSC apparatus (STA409PC/3/H Luxx). IR spectra were taken with a Perkin-Elmer Spectrum One Fourier transform infrared spectrometer as KBr pellets. NMR spectra were collected on a Bruker AC-250 MHz or a Bruker AV-400 MHz spectrometer.

Dimethyl *meso*-Galactarate.³⁵ *meso*-Galactaric acid (25 g) was refluxed with methanol and concentrated sulfuric acid overnight. The product was purified by recrystallization and dried under vacuum (14.4 g). Yield: 51%. ES/MS: m/z 261.0582 $[\text{M}+\text{Na}]^+$. ¹H NMR (D_2O): δ 4.60 (s, 2H), 4.08 (s, 2H), and 3.81 (s, 6H). ¹³C NMR ($\text{DMSO}-d_6$): δ 174.07, 71.14, 70.21, 51.40.

D-Mannaro-1,4:6,3-dilactone.³⁶ A mixture of D-mannitol (30 g), concentrated nitric acid (85 mL) and water (20 mL) was heated at 60 °C for 15 min until the evolution of gas was noticed. Next, the mixture was cooled with an ice bath until the vigorous formation of NO_2 (g) slowed. The reaction was then stirred at 60 °C for 4 h and then at 85 °C for 30 min. After evaporation of solvent under reduced pressure, diethyl ether (20 mL) was added to the viscous residue and stored at 4 °C overnight. After evaporation of ether under reduced pressure, the product was recrystallized from ethanol and filtered (3.0 g). Yield: 11%. ES/MS: m/z 175.0249 $[\text{M}+\text{H}]^+$. ¹H NMR ($\text{DMSO}-d_6$): δ 6.43 (s, 2H), 5.02 (d, 2H), and 4.78 (d, 2H). ¹³C NMR ($\text{DMSO}-d_6$): δ 173.92, 75.57, 69.07.

Polymerization. Each polymer was synthesized through condensation polymerization of esterified D-glucaric acid (D), dimethyl *meso*-galactarate (G), or D-mannaro-1,4:6,3-dilactone (M) with diethylenetriamine (1), triethylenetetramine (2), tetraethylenepentamine (3), or pentaethylenhexamine (4) in methanol at room temperature as detailed below.^{35,37} The poly(D-glucaramidoamine)s (D1–D4) were synthesized

(33) Jonassen, H. B.; Bertrand, J. A.; Groves, F. R.; Stearnes, R. I. *J. Am. Chem. Soc.* **1957**, *79*, 4279–4282.

(34) Kiely, D. E.; Chen, L.; Lin, T. H. *J. Am. Chem. Soc.* **1994**, *116*, 571–578.

(35) Kiely, D. E.; Chen, L.; Lin, T. H. *J. Polym. Sci. A: Polym. Chem.* **2000**, *38*, 594–603.

(36) Linstead, R. P.; Owen, L. N.; Webb, R. F. *J. Chem. Soc.* **1953**, 1225–1231.

(37) Ogata, N.; Sanui, K.; Hosoda, Y.; Nakamura, H. *J. Polym. Sci., Polym. Chem. Ed.* **1976**, *14*, 783–792.

as previously described.²² After polymerization, each product was dissolved in ultrapure water, exhaustively dialyzed to purity in a Spectra Por 1000 molecular weight cutoff membrane, and then lyophilized to dryness with a Flexi-dry MP lyophilizer. The solid products (Scheme 1) were of a white (**D1–D4** and **G1–G4**) or light yellow (**M1–M4**) color.

Poly(galactaramidodiethyleneamine) (G1). Diethylenetriamine (0.043 g, 0.42 mmol) was mixed with dimethyl *meso*-galactarate (0.10 g, 0.42 mmol, in 8.40 mL of methanol) and stirred at room temperature for 24 h. Yield: 0.09 g, 0.34 mmol, 81%. mp: 158.4 °C (dec). IR (KBr): 3306 cm⁻¹ (O–H and N–H stretching), 2939 and 2850 cm⁻¹ (C–H stretching), 1651 cm⁻¹ (amide C=O stretching), 1539 cm⁻¹ (amide N–H bending), 1476 cm⁻¹ (CH₂ scissoring), 1047 cm⁻¹ (amine C–N stretching). ¹H NMR (D₂O): δ 4.42 (s, 2H), 4.02 (s, 2H), 3.40 (br, 4H), 2.79 (br, 4H).

Poly(galactaramidotriethylenediamine) (G2). Triethylenetetramine hydrate (containing 20.42% H₂O, 0.15 g, 0.87 mmol) was mixed with dimethyl *meso*-galactarate (0.20 g, 0.84 mmol in 8.40 mL of methanol solution) and stirred at room temperature for 3 h. Yield: 0.07 g, 0.22 mmol, 26%. mp: 163.6 °C (dec). IR (KBr): 3307 cm⁻¹ (O–H and N–H stretching), 2939 and 2850 cm⁻¹ (C–H stretching), 1651 cm⁻¹ (amide C=O stretching), 1538 cm⁻¹ (amide N–H bending), 1434 cm⁻¹ (CH₂ scissoring), 1043 cm⁻¹ (amine C–N stretching). ¹H NMR (D₂O): δ 4.45 (s, 2H), 4.04 (s, 2H), 3.55 (br, 4H), 3.10 (br, 8H).

Poly(galactaramidotetraethylenetriamine) (G3). Dimethyl *meso*-galactarate (0.20 g, 0.84 mmol) was mixed with a methanol solution (5.60 mL) of triethylamine (0.43 g, 4.26 mmol) and tetraethylenepentamine pentahydrochloride (0.31 g, 0.83 mmol) and stirred at room temperature for 24 h. Yield: 0.23 g, 0.64 mmol, 76%. mp: 152.6 °C (dec). IR (KBr): 3251 cm⁻¹ (O–H and N–H stretching), 2939 and 2850 cm⁻¹ (C–H stretching), 1644 cm⁻¹ (amide C=O stretching), 1539 cm⁻¹ (amide N–H bending), 1476 cm⁻¹ (CH₂ scissoring), 1045 cm⁻¹ (amine C–N stretching). ¹H NMR (D₂O): δ 4.44 (s, 2H), 4.04 (s, 2H), 3.47 (br, 4H), 2.94 (br, 12H).

Poly(galactaramidopentaethylenetetramine) (G4). Dimethyl *meso*-galactarate (0.20 g, 0.84 mmol) was mixed with a methanol solution (5.60 mL) of triethylamine (0.52 g, 5.15 mmol) and pentaethylenhexamine hexahydrochloride (0.39 g, 0.86 mmol) and stirred at room temperature for 48 h. Yield: 0.12 g, 0.30 mmol, 35%. mp: 146.6 °C (dec). IR (KBr): 3364 cm⁻¹ (O–H and N–H stretching), 2939 and 2850 cm⁻¹ (C–H stretching), 1643 cm⁻¹ (amide C=O stretching), 1542 cm⁻¹ (amide N–H bending), 1476 cm⁻¹ (CH₂ scissoring), 1046 cm⁻¹ (amine C–N stretching). ¹H NMR (D₂O): δ 4.43 (s, 2H), 4.03 (s, 2H), 3.41 (br, 4H), 2.81 (br, 16H).

Poly(D-mannaramidodiethyleneamine) (M1). Diethylenetriamine (0.12 g, 1.16 mmol) was mixed with D-mannaro-1,4:6,3-dilactone (0.20 g, 1.15 mmol, in 5.75 mL of methanol) and stirred at room temperature for 24 h. Yield: 0.21 g, 0.76 mmol, 66%. mp: 140.3 °C (dec). IR (KBr): 3306 cm⁻¹ (O–H and N–H stretching), 2941 and 2850 cm⁻¹ (C–H stretching), 1652 cm⁻¹ (amide C=O stretching), 1548 cm⁻¹ (amide N–H bending), 1434 cm⁻¹ (CH₂ scissoring), 1048 cm⁻¹ (amine C–N stretching). ¹H NMR (D₂O): δ 4.22 (s, 2H), 3.94 (s, 2H), 3.42 (br, 4H), 2.88 (br, 4H).

Poly(D-mannaramidotriethylenediamine) (M2). Triethylenetetramine hydrate (containing 20.42% H₂O, 0.21 g, 1.16 mmol) was mixed with D-mannaro-1,4:6,3-dilactone (0.20 g, 1.15 mmol, in 7.67 mL of methanol) and stirred at room temperature for 48 h. Yield: 0.33 g, 1.03 mmol, 90%. mp: 146.6 °C (dec). IR (KBr): 3364 cm⁻¹ (O–H and N–H stretching), 2939 and 2850 cm⁻¹ (C–H stretching), 1643 cm⁻¹ (amide C=O stretching), 1539 cm⁻¹ (amide N–H bending), 1435 cm⁻¹ (CH₂ scissoring), 1099 cm⁻¹ (amine C–N stretching). ¹H NMR (D₂O): δ 4.20 (s, 2H), 3.92 (s, 2H), 3.38 (br, 4H), 2.75 (br, 8H).

Poly(D-mannaramidotetraethylenetriamine) (M3). D-Mannaro-1,4:6,3-dilactone (0.15 g, 0.86 mmol) was mixed with a methanol solution (5.75 mL) of triethylamine (0.43 g, 4.26 mmol) and tetraethylenepentamine pentahydrochloride (0.39 g, 0.86 mmol) and stirred at room

temperature for 80 h. Yield: 0.09 g, 0.26 mmol, 30%. mp: 140.7 °C (dec). IR (KBr): 3306 cm⁻¹ (O–H and N–H stretching), 2942 and 2850 cm⁻¹ (C–H stretching), 1652 cm⁻¹ (amide C=O stretching), 1539 cm⁻¹ (amide N–H bending), 1435 cm⁻¹ (CH₂ scissoring), 1084 cm⁻¹ (amine C–N stretching). ¹H NMR (D₂O): δ 4.21 (s, 2H), 3.92 (s, 2H), 3.40 (br, 4H), 2.85 (br, 12H).

Poly(D-mannaramidopentaethylenetetramine) (M4). D-Mannaro-1,4:6,3-dilactone (0.15 g, 0.86 mmol) was mixed with a methanol solution (5.75 mL) of triethylamine (0.52 g, 5.15 mmol) and pentaethylenhexamine hexahydrochloride (0.39 g, 0.86 mmol) and stirred at room temperature for 72 h. Yield: 0.08 g, 0.19 mmol, 22%. mp: 140.6 °C (dec). IR (KBr): 3354 cm⁻¹ (O–H and N–H stretching), 2939 and 2850 cm⁻¹ (C–H stretching), 1651 cm⁻¹ (amide C=O stretching), 1545 cm⁻¹ (amide N–H bending), 1474 cm⁻¹ (CH₂ scissoring), 1084 cm⁻¹ (amine C–N stretching). ¹H NMR (D₂O): δ 4.22 (s, 2H), 3.94 (s, 2H), 3.40 (br, 4H), 2.80 (br, 16H).

II. Polymer and Polyplex Characterization.

Gel Permeation Chromatography (GPC). The molecular weight, polydispersity and the Mark–Houwink–Sakurada (MHS) parameter (α) for the polymers were measured with a Viscotek GPCmax Instrument equipped with a Viscotek GMPW_{XL} column coupled to a triple detection system (static light scattering, viscometry and refractive index). Mobile phase (0.5 M sodium acetate, pH 5.0) was prepared in ultrapure water containing 20% acetonitrile. Each sample (100 μ L, 10–15 mg/mL) was dissolved in the mobile phase, immediately injected onto the column, and eluted at 1.0 mL/min.

Gel Electrophoresis Shift Assays. The ability of **D1–D4**, **G1–G4**, **M1–M4**, L-PEI, and chitosan to bind pDNA was examined by gel electrophoresis at 60 V. Agarose gel (0.6%, w/v) containing ethidium bromide (0.06 μ g/mL) was prepared in TAE buffer (40 mM Tris-acetate, 1 mM EDTA). Plasmid DNA (gWiz-Luc) was purchased from Aldevron (Fargo, ND) and the tested polymers were dissolved in Gibco nuclease-free water (Carlsbad, CA). The solution of chitosan was prepared according to a reported procedure by dissolving the chitosan in an aqueous acetic acid solution.³¹ gWiz-Luc (10 μ L, 0.1 μ g/ μ L) was mixed with an equal volume of polymer at N/P ratios between 0 and 50 (N = polymer nitrogens that can be protonated, P = phosphate groups on pDNA) and incubated for 30 min before the addition of loading buffer (1 μ L, Blue Juice, Invitrogen, Carlsbad, CA). An aliquot (10 μ L) of each sample was subjected to gel electrophoresis.

Dynamic Light Scattering and Zeta Potential. Polyplex sizes and their zeta potential values were measured at 662.0 nm on a Zetapals dynamic light scattering instrument (Brookhaven Instruments Corporation, Holtsville, NY). gWiz-Luc (150 μ L, 0.02 μ g/ μ L) was incubated with each polymer (N/P = 30) for 1 h before diluting to 0.7 mL (1.4 mL for zeta potential measurements) with nuclease-free water. The results are reported as an average of 10 measurements.

Transmission Electron Microscopy (TEM). Polymer–DNA complexes were prepared at N/P = 30 as described above for the dynamic light scattering. Samples (5 μ L) were applied in duplicate to 400-mesh carbon-coated copper grids (EMS, Fort Washington, PA) and incubated for 60 s before the removal of excess liquid by blotting with filter paper. Samples were negatively stained with uranyl acetate (2%, w/v) for 90 s. TEM images were recorded with a JEOL JEM-1230 transmission electron microscope operated at 80 kV.

Competitive Displacement by Heparin. **D4**, **G4**, and **M4** were incubated with gWiz-Luc (1 μ g) at N/P = 20 for 30 min. A series of heparin solutions [200–600 μ g/mL of heparin ammonium salt from porcine intestinal mucosa (Sigma, St. Louis, MO)] were prepared by diluting aliquots of a heparin stock solution (3200 μ g/mL). The polyplex solutions were incubated with 10 μ L of each heparin solution above for 15 min. After the addition of loading buffer (1 μ L), an aliquot (10 μ L) of each sample was subjected to electrophoresis.

III. Cell Culture Experiments. It should be noted that for all of the transfection and viability experiments performed with each cell line [with the poly(glycoamidoamine)s and controls], the transfections and

analyses were completed on the same day, on the identical passage of cells, with the same batches of culture media, serum, antibiotic, pDNA, polymer, cell lysis reagent, luciferase substrate, and protein assay reagent. The homogeneity of all the materials used in these experiments is essential to obtain accurate and reproducible data.

Cell Transfection and Luciferase Assay. Media and supplements were purchased from Gibco (Carlsbad, CA). BHK-21, HeLa (human cervix adenocarcinoma), and HepG2 (human hepatocellular carcinoma) cells were purchased from ATCC (Rockville, MD). BHK-21 and HeLa cells were cultured according to ATCC specifications in Dulbecco's Modified Eagle Medium (DMEM) and HepG2 cells in Eagle's Minimum Essential Media (EMEM) in 5% CO₂ at 37 °C. The media were supplemented with 10% fetal bovine serum, 100 units/mg penicillin, 100 µg/mL streptomycin, and 0.25 µg/mL amphotericin. Transfections were performed in serum-free media (Opti-MEM).

All reagents were prepared in nuclease-free water. The solution of chitosan was prepared according to a reported procedure by dissolving the chitosan in an aqueous acetic acid solution.³¹ **D1–D4, G1–G4, M1–M4**, L-PEI, and chitosan (150 µL) were incubated with gWiz-Luc (150 µL, 0.02 µg/µL) at N/P = 5, 10, 15, 20, 25, and 30 at room temperature for 1 h prior to diluting with 900 µL of serum-free media (Opti-MEM, pH 7.2). Each cell line was cultured at the appropriate density in 24-well plates (BHK-21 and HeLa at 5 × 10⁴ cells/well; HepG2 cells at 1 × 10⁵ cells/well) and incubated for 24 h prior to polyplex exposure. Thus, polyplexes containing a total of 1 µg of pDNA were added to each well of cells. Although a consistent amount of pDNA was added, the amount of polymer to form the polyplex was increased (as denoted by an increase in the N/P ratio) to determine the dependency of the polymer amount on the transfection efficiency. Transfections were performed with each cell line and N/P ratio in triplicate with 300 µL of polyplex solution. Four hours after initial transfection, 800 µL of the normal supplemented culture media was added to each well. Twenty-four hours after transfection, the media was replaced with fresh supplemented media (1 mL). Forty-seven hours after transfection, cell lysates were analyzed for luciferase activity with Promega's luciferase assay reagent (Madison, WI). For each sample, light units were integrated over 10 s in duplicate with a luminometer (GENios Pro, TECAN US, Research Triangle Park, NC), and the average was utilized. The negative controls were untransfected cells and cells transfected with naked gWiz-Luc (1 µg in serum-free media).

β-Galactosidase Reporter Gene Transfections and in Situ Staining of HeLa Cells. HeLa cells were transfected by polyplexes formed with gWiz β-gal (containing the β-galactosidase reporter gene, Aldevron) and **D1–D4, G1–G4, M1–M4**, L-PEI, and chitosan respectively, using the protocol described above. Negative controls were untransfected HeLa cells and cells transfected with naked gWiz β-gal. Forty-seven hours after transfection, the cells were fixed by incubation with glutaraldehyde (0.25%, v/v) for 15 min and rinsed with 3 × 1 mL of phosphate buffered saline (PBS, pH = 7.4).³⁸ After exposure to 0.2% X-Gal substrate (Promega) for 2 h, the cells were incubated in PBS (1 mL), counted, and photographed at 10× magnification with a Nikon (Melville, NY) D1 × 35 mm camera.

Cell Viability. The viability profiles of cells were characterized by the amount of protein in cell lysates obtained 47 h after the transfection, using a Bio-Rad DC protein assay kit (Hercules, CA). The amount of protein was measured against a standard curve of bovine serum albumin (98%, Sigma) at various concentrations prepared in cell culture lysis buffer. The protein level of untransfected cells was used as a standard for normalizing the protein levels of the cells transfected with each polyplex type.

Inhibition Studies with Asialofetuin in HepG2 Cells. Polyplexes were formed with **D1–D4, G1–G4, M1–M4** and gWiz-luc at N/P = 5, 10, 15, and 30. Cells were plated and transfected with each polymer following a similar protocol detailed in the Cell Transfection and

Luciferase Assay section. Prior to transfection, the HepG2 cells were preincubated with asialofetuin (200 µL; 1 mg/mL in Opti-MEM media; Sigma) at 4 °C for 15 min, transfected with each polyplex solution (100 µL), and incubated at 37 °C and 5% CO₂ for the duration of the experiment. Two hours after transfection, the Opti-MEM was removed, the cells rinsed with PBS (1 mL), and supplemented EMEM (1 mL) was added to each well. Twenty-two hours later, the media was replaced with fresh EMEM (1 mL). Forty-seven hours after transfection, the cells were lysed and analyzed for viability and luciferase activity as described above.

Heparin Competition Studies with HeLa Cells. Polyplexes were formed with **D1–D4, G1–G4, M1–M4** and gWiz-Luc at N/P = 20. Cells were plated and transfected following a similar protocol detailed for the Luciferase Assay. The negative controls in this experiment were untransfected HeLa cells and cells transfected with naked gWiz-Luc. Prior to transfection, the HeLa cells were preincubated with heparin-containing Opti-MEM (200 µL; 1, 10, 20, 50, and 100 µg/mL in Opti-MEM) at 4 °C for 15 min before the addition of polyplex solution in Opti-MEM (100 µL). Thus, the final concentrations of heparin used in the competition studies were 0.67, 6.67, 13.3, 33.3, and 66.7 µg/mL, respectively. The cells were incubated at 37 °C and 5% CO₂ for the duration of the experiment. Two hours after transfection, the Opti-MEM solution was removed, the cells were rinsed with PBS (1 mL), and fresh supplemented DMEM (1 mL) was added. Twenty-two hours later, the cells were recharged with DMEM (1 mL). Forty-seven hours after transfection, the cells were lysed and analyzed for viability and luciferase activity as described above.

The stability of the polyplexes prepared from **D1–D4, G1–G4**, and **M1–M4** in the experiment above was examined in the presence of heparin via gel electrophoresis. gWiz-Luc (10 µL, 0.1 µg/µL) was incubated with an equal volume of polymer solution at N/P = 20 for 30 min before the addition of heparin (10 µL of a 100 or 200 µL solution). The final concentration of heparin in this experiment was 33.3 and 66.7 µg/mL. This mixture was further incubated for another 40 min. Aliquots (10 µL) of the polyplex-heparin solutions were electrophoresed. This experiment verified the stability of the polyplexes at the experimental heparin concentrations in the cell culture experiments.

Results and Discussion

Synthesis and Characterization of Polymers. In an effort to design novel polymeric DNA carriers that are both nontoxic and highly efficacious, a series of carbohydrate-based comonomers were synthesized and polymerized with a series of di-primary amines. A library of polymers has been developed to gain an understanding of how subtle chemical changes affect the numerous processes involved with the intracellular delivery of nucleic acids. In a previous investigation, we described the synthesis of a family of poly(D-glucaramidoamine)s and found that the systematic placement of a D-glucarate (**D**) moiety within a PEI-like backbone significantly reduced the polymer cytotoxicity.²² In addition, a trend was observed where the gene expression increased as the amine number between the D-glucarate monomers increased. Furthermore, it was discovered that a particular analogue, **D4**, retained a similar delivery efficiency profile to L-PEI without any toxic effects.²² In the present study, we sought to examine if this trend held true when D-glucarate was substituted with other carbohydrate derivatives and thus, two additional polymer families, poly(galactaramidoamine)s and poly(D-mannaramidoamine)s, were synthesized. The three series of poly(glycoamidoamine)s have enabled us to systematically examine whether subtle chemical changes such as the hydroxyl stereochemistry and the amine number affect the overall toxicity and DNA delivery efficiency in a variety of mammalian cell lines.

(38) MacGregor, G.; Caskey, C. *Nucleic Acids Res.* **1989**, *17*, 2365.

Table 1. MHS Parameter (α), Molecular Weight (M_w), Polydispersity (M_w/M_n), and Degree of Polymerization (n) Data for the Poly(glycoamidoamine)s

polymer	α	M_w (kDa)	M_w/M_n	n
D1	0.68	3.0	2.0	11
D2	0.67	3.4	1.4	11
D3	0.64	3.9	1.4	11
D4	0.61	4.9	1.6	12
G1	0.66	3.1	1.9	11
G2	0.63	4.4	1.7	14
G3	0.68	5.1	1.5	14
G4	0.64	4.6	1.5	11
M1	0.87	2.9	1.2	11
M2	0.64	4.2	1.9	13
M3	0.97	4.6	1.2	12
M4	0.73	5.6	1.2	14

The carbohydrate monomers were synthesized according to previously reported procedures^{22,34–36} and polymerized with a family of monomers that contain between 1 and 4 secondary amine units (Scheme 1). The poly(D-glucaramidoamine)s **D1–D4**, the poly(galactaramidoamine)s **G1–G4**, and the poly(D-mannaramidoamine)s **M1–M4** were synthesized via polymerization of esterified D-glucuric acid (**D**), dimethyl *meso*-galactarate (**G**), and D-mannaro-1,4:6,3-dilactone (**M**) with diethylenetriamine (**1**), triethylenetetramine (**2**), tetraethylenepentamine (**3**), or pentaethylenhexamine (**4**) in methanol at room temperature to create twelve specific polymer structures with defined chemical properties. It has been shown that carbohydrate ester and lactone monomers have great reactivity toward amines and can be polymerized with diamines without a catalyst under mild conditions. The presence of electron withdrawing hydroxyl groups on the α, α' carbons of diesters or dilactones activates the carbonyl groups toward nucleophilic attack by amines.^{35,37,39,40} This reaction has been found to proceed considerably faster in protic solvents.^{37,39,40} Previous investigations indicate that a similar polymerization mechanism occurs for carbohydrate ester and lactone monomers in the formation of polyamides. Hoagland and Kiely et al. have both performed kinetic studies on these species and have found that the aminolysis reaction is accelerated for linear carbohydrate esters due to the formation of a five-membered lactone ring intermediate. The amide is formed when ring-opening of the lactone occurs due to amine attack on the carbonyl group.^{40,41} Thus, the mixture of the methyl-D-glucurate lactones and the dimethyl-D-glucurate comonomers were utilized in the polymerization reaction without further separation.

Ring-opening polymerization of D-mannaro-1,4:6,3-dilactone was facilitated by nucleophilic attack on the dilactone with the various primary amine monomers under similar conditions.⁴² In all of the reactions with tetraethylenepentamine and pentaethylenhexamine, triethylamine was added to liberate the hydrochloride salts of the monomers to promote monomer coupling. The polymerization of the poly(glycoamidoamine)s was monitored via GPC containing a triple detection system (static light scattering, viscometry and refractive index) (Table 1). The reaction conditions were optimized to yield polymers with similar degrees of polymerization (Table 1, n values

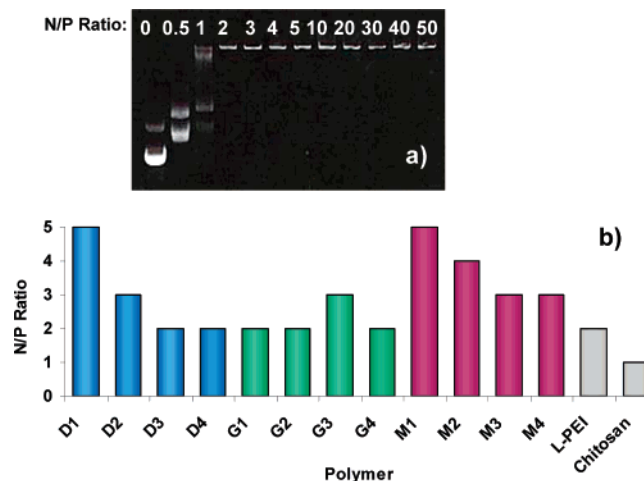


Figure 3. (a) Agarose gel electrophoretic pDNA binding shift assay for **G1**. The N/P ratios of polymer–pDNA mixing are shown. (b) The N/P ratio of pDNA binding for **D1–D4**, **G1–G4**, **M1–M4**, L-PEI, and chitosan.

between 11 and 14), ensuring that the biological properties of these polymers could be accurately compared within and between each family of structures. This is important because previous investigations have observed that variations in the degrees of polymerization can lead to significant differences in the delivery efficiency and cytotoxicity profiles of materials with identical chemical structures.^{25,43}

The MHS α values of the poly(glycoamidoamine)s were calculated from the MHS equation ($[\eta]=MK^\alpha$) by plotting the logarithm of the intrinsic viscosity versus the logarithm of the molecular weight distribution. In solution, α values between 0.5 and 0.8 generally indicate randomly coiled linear polymers and α values in the range of 0.8–1.0 denote linear, stiff-chain structures. The α values of the poly(glycoamidoamine)s were in the range of 0.6–1.0 indicating these polymers have low degrees of branching. This suggests that polymerization may be occurring predominantly through the terminal primary amines with monomers **1–4**, with a low degree of branching off of the secondary amines.⁴⁴ As shown, **D1–D4** and **G1–G4** all exhibit linear, randomly coiled solution structures (Table 1, $\alpha = 0.61–0.68$). However, the poly(D-mannaramidoamine)s generally displayed higher α values, indicating a more stiff-chain character. This observation may be related to the stereoregular structures that are created upon polymerization of the symmetric D-mannarate monomer [unlike the poly(D-glucaramidoamine)s and poly(galactaramidoamine)s, which polymerize in an atactic manner]. The correlation between stereoregularity and increased polymer chain stiffness has been previously observed with polystyrenes and various polyvinyl ethers.⁴⁵

The Structural Effects on pDNA Binding and Compaction. Gel shift assays reveal that the binding affinities observed by combining each poly(glycoamidoamine) with pDNA are dependent on the N/P ratio (the ratio of the number of amines within the polymer/phosphate groups on the pDNA). As shown in Figure 3a, stable binding between **G1** and pDNA began at

(39) Ogata, N.; Hosoda, Y. *J. Polym. Sci., Polym. Chem. Ed.* **1975**, *13*, 1793–1801.

(40) Viswanathan, A.; Kiely, D. E. *J. Carbohydr. Chem.* **2003**, *22*, 903–918.

(41) Hoagland, P. D. *Carbohydr. Res.* **1981**, *98*, 203–208.

(42) Hashimoto, K.; Wibullucksanakul, S.; Matsuda, M.; Okada, M. *J. Polym. Sci. A: Polym. Chem.* **1993**, *31*, 3141–3149.

(43) (a) Zelikin, A. N.; Putnam, D.; Shastri, P.; Langer, R.; Izumrudov, V. A. *Bioconjugate Chem.* **2002**, *13*, 548–553. (b) Sato, T.; Ishii, T.; Okahata, Y. *Biomaterials* **2001**, *22*, 2075–2080.

(44) McC. Arnett, E.; Miller, J. G.; Day, A. R. *J. Am. Chem. Soc.* **1951**, *73*, 5393–5395.

(45) (a) Kern, R. J.; Hawkins, J. J.; Calfee, J. D. *Makromol. Chem.* **1963**, *66*, 126–132. (b) Inoue, T.; Ryu, D. S.; Osaki, K.; Takebe, T. *J. Polym. Sci. B: Polym. Phys.* **1999**, *37*, 399–404.

an N/P ratio of 2, where migration of the pDNA with the electrophoretic field is inhibited due to effective binding and charge neutralization. Figure 3b reveals that all of the poly-(glycoamidoamine)s bind and charge neutralize pDNA at N/P ratios between 2 and 5, which is similar to both L-PEI and chitosan (N/P = 2 and 1, respectively). As generally observed in Figure 3b, as the number of amines increases between the carbohydrate comonomers, a decrease in the N/P ratio of binding is observed in most cases. This observation indicates that the polymer–pDNA binding becomes more stable with an increase in the number of secondary amines between the carbohydrate groups. A similar effect has been observed by Plank et al. in a series of branched cationic peptides where an increase in DNA binding affinity was observed with an increase in the number of cationic groups between neutral residues.⁴⁶

In general, the galactarate (**G1**, **G2**, **G4**) and the D-glucarate (**D2**–**D4**) structures bound pDNA at lower N/P values than their analogous structures in the D-mannarate (**M1**–**M4**) series (Figure 3b). This observation suggested that the stereochemistry of hydroxyl groups possibly contributes to the binding strength between the polymers and pDNA. To further examine the effect of the hydroxyl stereochemistry on polyplex stability, a heparin competitive displacement assay was performed.⁴⁷ When polyplexes formed with each polymer are exposed to solutions containing heparin, this polyanion competes with the complexed pDNA (also a polyanion) for polymer binding. Thus, the stability of the polyplexes can be qualitatively determined by observing the concentration at which heparin begins to release the pDNA from the polyplex (the higher the heparin concentration needed to release the pDNA, the more stable the polymer–pDNA interaction). As shown in Figure 4c, it was noticed that the polyplex formed with **M4** and pDNA started to dissociate at the lowest heparin concentration of 240 $\mu\text{g}/\text{mL}$. However, the polyplexes formed with **D4** (Figure 4a) and **G4** (Figure 4b,d) did not begin to dissociate until higher heparin concentrations of 340 and 440 $\mu\text{g}/\text{mL}$ respectively suggesting that **G4** binds pDNA with the highest affinity. This result further supports the data obtained from the gel shift assays that the stereochemistry of the hydroxyl groups influences the poly(glycoamidoamine)–pDNA binding strength and that the poly(galactaramidoamine)s appear to have a higher DNA binding affinity (where **G4** > **D4** > **M4**).

It is well known, particularly for aminoglycoside antibiotics, that changes in the carbohydrate stereochemistry of oligoaminosaccharides can cause diverse interactions with nucleic acids.⁴⁸ The disparity in binding affinity is primarily induced by several hydrogen bonding interactions such as hydroxyl-phosphodiester, hydroxyl-amine, and hydroxyl-carbonyl.⁴⁹ Here, the poly-(galactaramidoamine)s seem to facilitate stronger interactions with pDNA. Jeffrey et al. have reported that *meso*-galactaric acid promotes exceptionally strong intermolecular hydrogen bonds (as revealed in the *meso*-galactaric acid crystal structure) as compared to D-glucaric and D-mannaric acid.⁵⁰ In support of this, the poly(galactaramidoamine)s possess higher melting

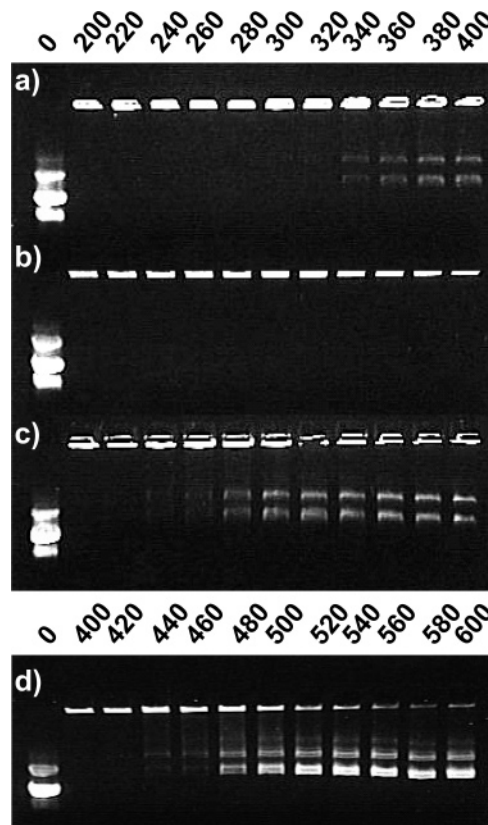


Figure 4. Determination of relative binding affinity of (a) **D4**, (b) **G4**, and (c) **M4** with pDNA as determined by competitive displacement with heparin. The concentration of heparin ($\mu\text{g}/\text{mL}$) that is required to release pDNA from the polyplexes is shown. **G4** required a higher concentration than **D4** and **M4** to release pDNA as shown in (d). The first lane in each gel is the uncomplexed pDNA control.

points than their corresponding D-glucarate or D-mannarate analogues indicating stronger intermolecular hydrogen bonding (data in Experimental Section). Stronger hydrogen bonding between the *meso*-galactarate units and pDNA may contribute to the increase in binding affinity of these structures over the D-glucarate and D-mannarate polymers. Also, the stiffer-chain properties of the poly(mannaramidoamine)s may contribute to their weaker binding affinity with pDNA (decreased chain flexibility could impair polymer binding around the helical DNA structure).

The efficient compaction of pDNA into nanoparticles is an essential process that mediates the endocytosis of polyplexes, where cells typically uptake particles ranging from about 50 to several hundred nanometers.⁵¹ Previous investigations have shown that the polycation structure contributes to effective pDNA compaction. Jones et al. have shown that changes in the chemical groups within a series of poly(amidoamine)s alter the pDNA binding affinity, the size, and colloidal stability of the subsequent polyplexes.⁵² To examine the size of the nanoparticles formed with each poly(glycoamidoamine) and pDNA, dynamic light scattering measurements were performed on polyplex solutions in nuclease-free water. Figure 5 shows that all of the polymers are able to compact pDNA into nanoparticles

(46) Plank, C.; Tang, M. X.; Wolf, A. R.; Szoka, F. C. *Hum. Gene Ther.* **1999**, *10*, 319–332.

(47) Hwang, S. J.; Bellocq, N. C.; Davis, M. E. *Bioconjugate Chem.* **2001**, *12*, 280–290.

(48) Fourmy, D.; Recht, M. I.; Blanchard, S. C.; Puglisi, J. D. *Science* **1996**, *274*, 1367–1371.

(49) Sucheck, S. J.; Wong, C. H. *Curr. Opin. Chem. Biol.* **2000**, *4*, 678–686.

(50) Jeffrey, G. A.; Wood, R. A. *Carbohydr. Res.* **1982**, *108*, 205–211.

(51) Mukherjee, A.; Ghosh, R. N.; Maxfield, F. R. *Physiol. Rev.* **1997**, *77*, 759–803. (b) Garnett, M. C. *Crit. Rev. Ther. Drug Carr. Sys.* **1999**, *16*, 147–207.

(52) Jones, N. A.; Hill, I. R. C.; Stolnik, S.; Bignotti, F.; Davis, S. S.; Garnett, M. C. *Biochim. Biophys. Acta* **2000**, *1517*, 1–18.

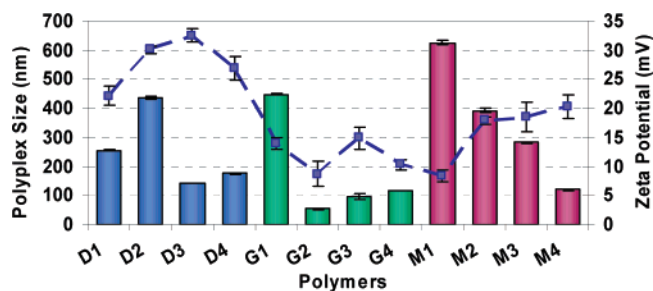


Figure 5. Polyplex size (bars) and the zeta potential (line) for the complexes formed with polymers **D1–D4**, **G1–G4**, and **M1–M4** and pDNA at $N/P = 30$.

in the size range to be endocytosed (between 54 and 625 nm). Generally, within each poly(glycoamidoamine) family, the structures with the lower amount of amines between the carbohydrate comonomers give rise to larger average particles suggesting that increasing the amine number yields smaller polyplexes (Figure 5). This result is particularly noticed with **M1–M4** where the polyplex size decreases systematically as the number of amines between the *D*-mannarate residues increases. The galactarate analogues (**G2–G4**) generally condense pDNA into the smallest nanoparticles, while the *D*-mannarate systems typically produce the largest average polyplexes. These studies imply that both the number of amines and the hydroxyl stereochemistry mediate the compaction of pDNA and these results complement the data obtained from the gel electrophoretic binding studies. All of the polymers (with the exception of **M1**) yield polyplexes in a similar size range to the positive control polymers, L-PEI (yields polyplexes between 80 and 150 nm)²⁷ and chitosan (polyplex sizes between 100 and 500 nm).³¹ These results indicate that the poly(glycoamidoamine)s show promise as viable nucleic acid delivery vehicles because of their effective pDNA compaction properties.

Zeta potential measurements were conducted on aqueous solutions containing the nanoparticles formed with each polymer and pDNA at $N/P = 30$ to determine the charge on the polyplex surface. Figure 5 reveals that all of the polyplexes are positively charged where the galactarate series generally form polyplexes with the lowest zeta potential values and the *D*-glucarate series the highest. The positive charge of the polyplexes facilitates nonspecific interactions with negatively charged cell surface proteins that trigger cellular uptake. The low zeta potential values of the poly(galactaramidoamine) polyplexes may be related to the stronger intermolecular hydrogen bonding between the polymers and pDNA.

The morphology of the polyplexes formed with **D4**, **G4**, and **M4** and pDNA was characterized by transmission electron microscopy (TEM). In the previous study, we found that **D4** compacts pDNA into polyplexes with viral-like size and shape (Figure 6a).²² Polymers **G4** and **M4** (Figure 6b,c, respectively) also maintain the ability to compact pDNA into nanoparticles. The polyplexes formed with each analogue reveal similar morphologies; however, **G4** generally forms smaller particles with pDNA than **M4** and **D4**. This result is consistent with the dynamic light scattering data, and further supports our observations that the hydroxyl stereochemistry within the carbohydrates affects the binding and compaction of pDNA with poly(glycoamidoamine)s.

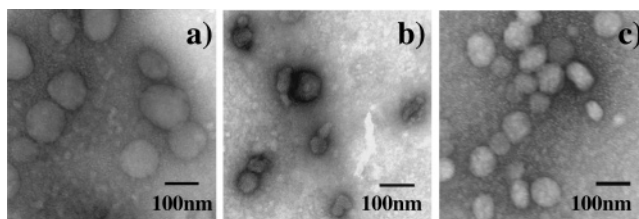


Figure 6. Transmission electron micrographs of polyplexes formed with pDNA at $N/P = 30$. (a) **D4**, (b) **G4**, and (c) **M4**. The polyplexes were negatively stained with uranyl acetate.

Viability and Gene Delivery Studies. The cell viability and efficiency of reporter gene expression with carriers **D1–D4**, **G1–G4**, **M1–M4**, L-PEI and chitosan were examined in three mammalian cell lines: BHK-21, HeLa, and HepG2 cells. As shown in Figure 7, high viability was retained after cellular exposure to polyplexes formed with all of the synthetic vectors even at the N/P ratios required for maximum gene expression [N/P ratios between 20 and 30 for all of the poly(glycoamidoamine)s and $N/P=5$ for L-PEI and chitosan]. This result implies that the poly(glycoamidoamine)s are nontoxic even at high N/P ratios. The cell viability profiles were all 90% or greater with **D1–D4**, **G2–G4**, and **M1–M4** in BHK-21 and HeLa cells (with the exception of **G1**). The cytotoxicity with HepG2 cells was also very low where 80% or greater viability was observed with most of the synthetic structures. Only polymers **M2** and **M3** reveal slightly elevated cytotoxicity (with HepG2 cells); however, the viability was still greater than 70%. Overall, it was discovered that the cell viability did not decrease with increasing amine density. The polymers presented here retain the biocompatible properties characteristic of chitosan even though many of the systems contain a significantly higher density of amine groups. L-PEI displays elevated cytotoxicity where complete cell death was observed at N/P ratios of 15 and above. At the N/P ratio of maximum gene expression ($N/P = 5$ for L-PEI), cell viability was still lower (only about 50% with BHK-21 and HeLa, and 70% with HepG2 cells) than the structures synthesized for this study. The low toxicity results obtained for the poly(glycoamidoamine)s are significant because the most efficient cellular delivery vehicles, such as L-PEI, typically display high cytotoxicity, which has hampered their clinical use.

The ability of each polymeric vector to deliver pDNA was examined via luciferase reporter gene expression experiments at N/P ratios from 5 to 30 with the three cell lines. This experiment allows the quantification of the average luciferase gene expression per well of cells and is a method commonly used to evaluate the efficacy of gene delivery vehicles in vitro. After 47 h of exposure to polyplexes formed with the poly(glycoamidoamine)s and the positive control polymers (L-PEI and chitosan), the cells were lysed and analyzed for luciferase activity. All of the new poly(glycoamidoamine)s were able to deliver pDNA. Within each family, the derivatives containing four secondary amines between the carbohydrates (**D4**, **G4**, and **M4**) displayed the highest gene expression values (Figure 8). This result indicates that the number of amine units plays a role in the ability of the polymers to deliver pDNA, where an increase in the amine number enhances the delivery efficiency.

For the galactarate and *D*-glucarate series, similar luciferase expression profiles are observed with all three cell lines. In BHK-21 cells, luciferase expression increases as the amine

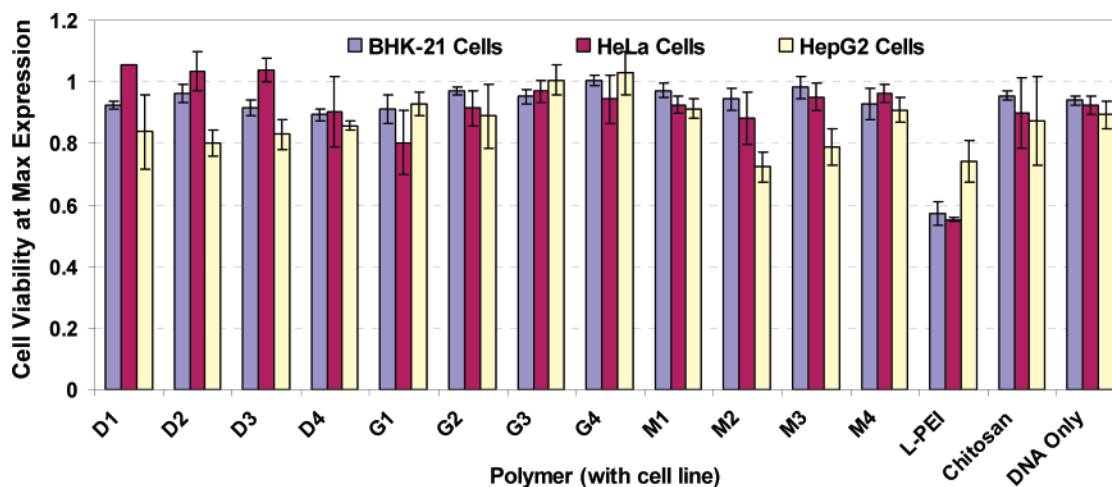


Figure 7. Cell viability at maximum gene expression for BHK-21, HeLa, and HepG2 cells transfected with polyplexes formed with polymers **D1–D4**, **G1–G4**, **M1–M4**, L-PEI, chitosan, and uncomplexed pDNA. The cell viability values were normalized to untransfected cells. The data are reported as a mean \pm standard of deviation of three replicates.

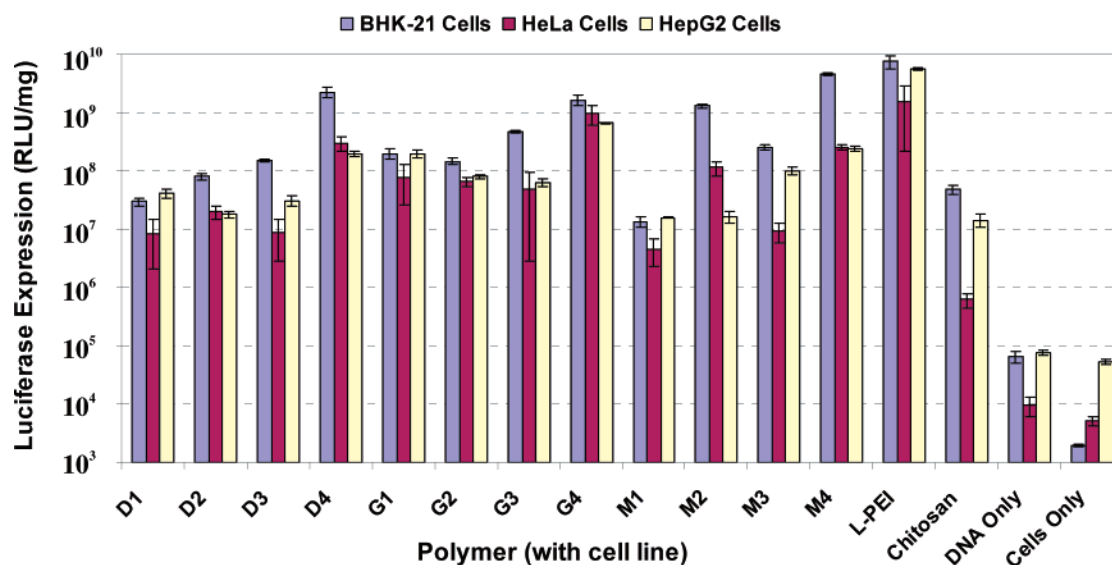


Figure 8. Maximum luciferase gene expression observed with polyplexes formed with **D1–D4**, **G1–G4**, **M1–M4**, and the controls L-PEI, chitosan, uncomplexed pDNA, and untransfected cells. The gene expression values are shown as relative light units (RLU) per milligram of protein. The N/P ratios of maximum gene expression for **D1–M4** were between 20 and 30 and for L-PEI and chitosan at an N/P ratio of 5. The data are reported as a mean \pm standard of deviation of three replicates.

number between the galactarate or D-glucarate residues increases (Figure 8). In HeLa cells, luciferase expression is higher with polymers **D2**, **G2**, **D4**, and **G4** polymers than with **D1**, **G1**, **D3**, and **G3**, denoting that the delivery trends are not consistent will all cell lines. In HepG2 cells, a slight decrease in gene expression is noticed with **G1–G3** and **D1–D3**, however, a significant enhancement in expression is observed with **G4** and **D4**. For the poly(D-mannaramidoamine)s, luciferase expression is considerably higher with the **M2** and **M4** analogues than with **M1** and **M3** in BHK-21 and HeLa cells. This effect may be due to the stiff-chain properties of **M1** and **M3** as determined by visometry measurements (Table 1, $\alpha > 0.8$). Stiffer polymers may not bind pDNA as strongly as compared to flexible systems and thus the lower delivery efficiency may be due to the formation of less stable polyplexes with these vectors. Moreover, in HepG2 cells, gene expression increases as the number of amines increases between the D-mannarate residues.

The galactarate polymer series generally presented higher gene expression profiles than the D-glucarate or D-mannarate

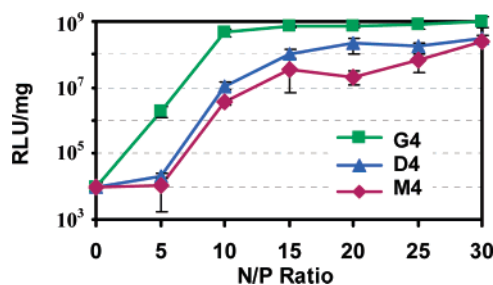


Figure 9. Effect of hydroxyl stereochemistry on luciferase gene expression (RLU/mg) in HeLa cells with polyplexes formed with **G4**, **D4**, and **M4** at N/P ratios between 0 (pDNA only) and 30. The data are reported as a mean \pm standard of deviation of three replicates.

analogues in all three cell lines with a few exceptions. As highlighted in Figure 9 for polymers **G4**, **D4**, and **M4**, this result was more significant with the human cell lines (HeLa and HepG2). In this experiment, polyplexes were formed at several N/P ratios between 5 and 30 by adding an increasing amount of polymer to a fixed amount of pDNA. At all polymer and

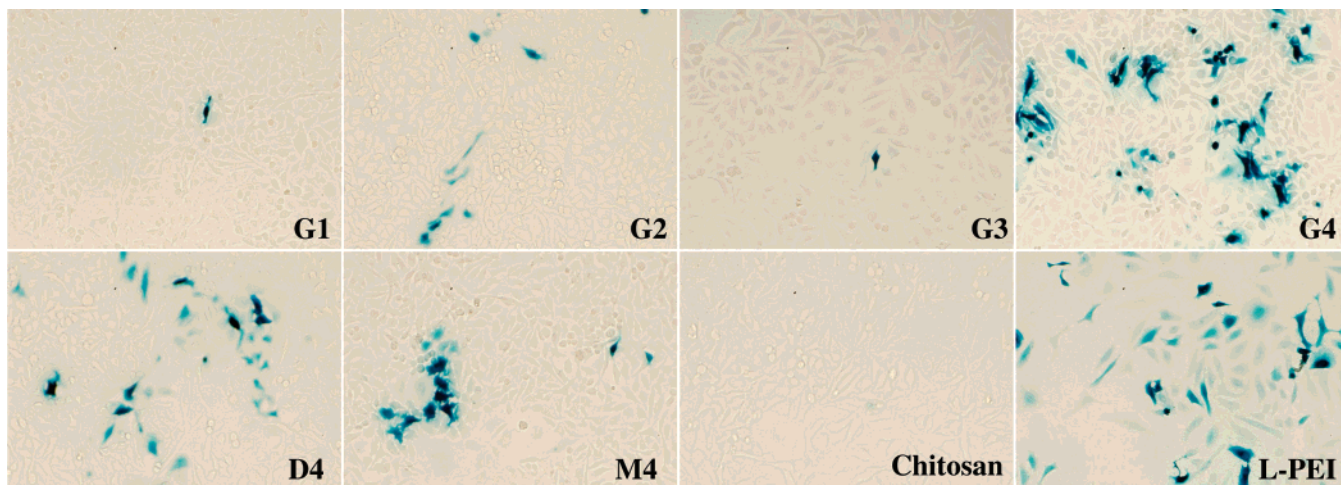


Figure 10. HeLa cells transfected with polyplexes formed at an N/P ratio of 20 with polymers **G1–G4**, **D4**, **M4**, chitosan and L-PEI complexed to pDNA containing the β -galactosidase reporter gene. As shown, cells positive for β -galactosidase stain blue.

pDNA N/P ratios, **G4** reveals significantly higher gene expression in HeLa cells than the other saccharide analogues (Figure 9 shows that the vector delivery efficiency is **G4** > **D4** > **M4**). The same trend was observed with HepG2 cells. This observation may be related to the affinity of pDNA binding where the trend observed was **G4** > **D4** > **M4** (Figure 4). However, it was noticed with BHK-21 cells (hamster kidney) that the gene expression trend was completely opposite than that observed in the human cell lines (**M4** > **D4** > **G4**). These data imply that both the binding affinity and the host cell type will most likely affect the selection of efficacious nucleic acid delivery vectors because the gene expression results with the poly-(glycoamidoamine)s are not consistent in all three cell lines.

The luciferase reporter gene assay quantitates the luciferase expression averaged over the total number of cells exposed to solutions of the polyplexes containing 1 μ g of pDNA. However, this assay does not directly determine the number of cells successfully transfected. In a complementary experiment, β -galactosidase reporter gene delivery experiments in HeLa cells were performed to identify the actual number of cells that successfully uptake the polyplexes and express the reporter genes (cells stain blue). As pictured in Figure 10, **G2** and **G4** generally transfect more HeLa cells than polymers **G1** and **G3**. This trend is also observed with the D-glucarate and the D-mannarate series (data not shown). To quantitate the number of successfully transfected cells, the average number of stained HeLa cells was counted in each well (the average percentages of transfected HeLa cells for **D4**, **G4**, and **M4**, L-PEI, and chitosan were: 8.3%, 16%, 4.7%, 37%, and 0.1% respectively). **G4** transfects almost twice as many HeLa cells as **D4** and three times as many HeLa cells as **M4** at an N/P ratio of 20, which is consistent with the results of the luciferase gene expression assays in HeLa cells (**G4** > **D4** > **M4**, Figure 9) and the pDNA binding data (**G4** > **D4** > **M4**, Figure 4). These results again indicate that the hydroxyl stereochemistry affects the transfection efficiency of genetic material.

The hydroxyl stereochemistry within carbohydrates can play a significant role in the cellular uptake of glycoside species. For example, it is widely known that liver hepatocytes (i.e. HepG2 cells) that contain the asialoglycoprotein receptor, recognize and bind to saccharides that contain β -D-galactose moieties.⁵³ These species signal cellular uptake through receptor-

mediated endocytosis. In an effort to further comprehend the higher transfection efficiency resulting with the galactarate polymers, experiments were completed to determine if the higher uptake is due to asialoglycoprotein receptor-mediated endocytosis. Competitive inhibition studies with HepG2 cells were performed by adding polyplexes formed with **G4**, **D4**, and **M4** to cellular media supplemented with asialofetuin (free receptor protein) that would compete with the asialoglycoprotein receptor on the surface of HepG2 cells for polyplex binding.⁵⁴ Although a slight decrease in transfection was noted (data not shown) for all three of the polymers with media containing asialofetuin (as compared to the controls), the decrease was consistent with all three saccharide systems. This study confirmed that the preferential uptake noted for the galactarate polyplexes with HepG2 cells was not due to preferential uptake through the asialoglycoprotein receptor.

The general cellular uptake of cationic polyplexes is believed to occur through electrostatic binding of these systems with anionic cell surface proteins (proteoglycans) that subsequently trigger endocytosis.^{55,56} Proteoglycans consist of a central protein sequence that is linked to sulfated polysaccharide (glycosaminoglycan) residues that are responsible for such biological functions as cellular uptake, cellular signaling, and viral infection.⁵⁵ We hypothesized that the interaction of the polyplexes with cell surface polysaccharides plays a role in the transfection efficiency difference that is observed between the D-glucarate, *meso*-galactarate, and D-mannarate polymeric gene delivery vectors. To test this hypothesis, competitive inhibition assays were carried out with polyplexes formed with **D1–D4**, **G1–G4**, **M1–M4** and pDNA at N/P = 20 in media supplemented with free heparin, a common cell surface polysaccharide. Therefore, if gene expression decreases upon addition of free heparin, the polyplex uptake is triggered by glycosaminoglycan binding. A significant decrease in gene expression was noted with polyplexes formed with all of the synthetic polymers upon

- (53) (a) Zanta, M. A.; Boussif, O.; Adib, A.; Behr, J. P. *Bioconjugate Chem.* **1997**, *8*, 839–844. (b) Kunath, K.; von Harpe, A.; Fischer, D.; Kissel, T. *J. Controlled Release* **2003**, *88*, 159–172. (c) Lim, D. W.; Yeom, Y. I.; Park, T. G. *Bioconjugate Chem.* **2000**, *11*, 688–695.
 (54) Hwang Pun, S.; Davis, M. E. *Bioconjugate Chem.* **2002**, *13*, 630–639.
 (55) Mislick, K. A.; Baldeschwieler, J. D. *Proc. Natl. Acad. Sci. U.S.A.* **1996**, *93*, 12349–12354.
 (56) Ruponen, M.; Yla-Herttuala, S.; Urtti, A. *Biochim. Biophys. Acta* **1999**, *1415*, 331–341.

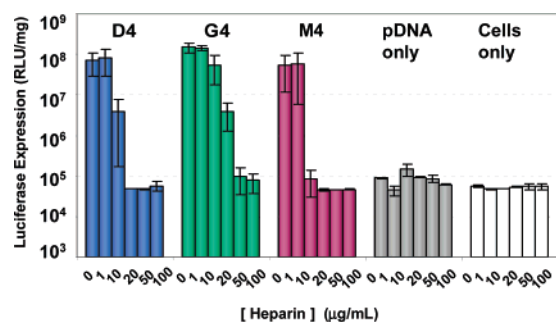


Figure 11. Heparin competitive inhibition assays completed with HeLa cells and polyplexes formed by complexing **D4**, **G4**, and **M4** with pDNA containing the firefly luciferase reporter gene. Cells transfected with naked pDNA and untransfected cells in the presence of heparin were the controls in this study. The data are reported as a mean \pm standard of deviation of two replicates.

the addition of between 10 and 100 $\mu\text{g/mL}$ heparin to the media. To confirm that the inhibition of polyplex uptake and gene expression was not due to polyplex dissociation by free heparin in the media, polyplexes formed with all of the poly(glycoamidoamine)s ($N/P = 20$) were incubated with the same heparin concentrations in the previous experiment and electrophoresed. Polyplex dissociation was not observed at the experimental heparin concentrations (no migration of the pDNA was noticed) therefore indicating that the decreased gene expression was due to a competitive inhibitory effect (down regulates polyplex uptake). This result suggests that the polyplexes formed with the poly(glycoamidoamine)s are endocytosed primarily through interaction with the cell surface glycosaminoglycans (particularly heparin), which is a similar mechanism in which viral delivery vehicles enter cells.

It was observed that polyplexes formed with the galactarate polymers revealed less of an inhibitory effect and higher gene expression profiles upon the addition of heparin than with D-glucarate or D-mannarate polyplexes. This was particularly noticed at heparin concentrations of 10 and 20 $\mu\text{g/mL}$. As highlighted in Figure 11, gene expression with **G4** is slightly reduced at 10 $\mu\text{g/mL}$, however, a larger reduction was noticed with **D4**, and a complete inhibition was observed with **M4** polyplexes. Moreover, with the addition of 20 $\mu\text{g/mL}$ of heparin, **G4** promoted a moderate level of gene expression while **D4** and **M4** completely failed to deliver the reporter gene. While the lack of inhibition with **G4** could be related to the lower zeta potential values (lower positive charge) noticed with **G4** polyplexes, the total order of binding affinities (**G4** > **D4** > **M4**) did not correlate with the zeta potential values observed (**D4** > **M4** > **G4**, Figure 5). Although these results could also indicate that the galactarate polyplexes participate in another pathway for cellular uptake, we believe the inhibitory effects observed are most likely due to the stronger pDNA binding affinity noticed with the galactarate systems (Figures 3 and 4).

The glycosaminoglycan heparin is present at various levels on cell surfaces and not only plays a role in polyplex binding and endocytosis but affects the release of the polymer from the pDNA (pDNA unpackaging).^{56,57} If the binding affinity of the polymer to pDNA is weak, the high local concentration of heparin that is presented to polyplexes bound to the cell surface may prematurely dissociate the polymer from the pDNA before

endocytosis, therefore decreasing cellular delivery and gene expression. However, if the polymer binding affinity is strong, many of the polyplexes may remain intact during the glycosaminoglycan binding event, be endocytosed, and polymer–pDNA dissociation may occur within the endosome, where an even higher local glycosaminoglycan concentration would be present. This hypothesis is supported by the competitive displacement experiments (Figure 4) that were completed by adding various concentrations of heparin to polyplexes formed with **G4**, **D4**, and **M4** polyplexes. These results are consistent with both the luciferase gene expression experiments and the β -galactosidase gene delivery experiments, which both reveal that the efficiency of gene expression and number of cells transfected correlate to the binding affinity (**G4** > **D4** > **M4**). These data suggest that the delivery efficiency of synthetic vectors is most likely dependent on the polymer–pDNA binding affinity. This study demonstrates that very subtle chemical changes (ie. the stereochemistry of one hydroxyl group in the polymer repeat unit) can significantly affect the pDNA binding affinity and efficacy of nucleic acid delivery.

Conclusion

A new library of poly(glycoamidoamine)s has been synthesized, characterized, and examined for their toxicity profiles and abilities to deliver pDNA in three mammalian cell lines. All of the polymers created for this study bind pDNA with varying affinities according to gel electrophoresis shift assays and electrophoretic competitive displacement experiments with heparin. Dynamic light scattering and TEM experiments reveal that all of the polymers compact pDNA into viral-sized polyplexes. Polymers **G1**–**G4** generally bind pDNA at the lowest N/P ratios and have the most efficient pDNA compaction properties. Cell culture experiments with BHK-21, HeLa, and HepG2 cells demonstrate that all of the poly(glycoamidoamine)s retain very low toxicity profiles (similar to chitosan) and the hydroxyl stereochemistry and amine number generally do not affect the observed cell viability. The positive control, L-PEI, reveals significantly lower cell viability profiles. These results indicate that the carbohydrate residues along a PEI-like backbone lower the toxicity associated with polymeric vectors.

Both the gene expression and the number of cells transfected by each type of polyplex is significantly affected by the hydroxyl stereochemistry and the number of amine units between the carbohydrate residues. In general, the galactarate polymers have the highest gene expression profiles. Additionally, β -galactosidase reporter gene experiments demonstrate that **G4** transfects twice as many HeLa cells as **D4** and three times as many cells as **M4**. In addition **D4**, **G4**, and **M4** all reveal the highest delivery efficiency in each respective carbohydrate polymer family, indicating that an increase in amine density enhances the delivery efficiency. These data are consistent with the binding profiles and may suggest that pDNA binding affinity affects the gene delivery efficiency. If the polymer–pDNA binding is weak, the high local concentrations of anionic glycosaminoglycans on the cell surface may prematurely dissociate the polyplexes during the cell surface binding event. This may release the pDNA from the polyplex due to competitive binding of the anionic cell surface polysaccharides with the cationic polymers. If the polymer has a higher pDNA binding affinity, the polyplexes may remain intact during glycosaminoglycan binding and endocytosis. Therefore, pDNA dissociation

(57) Zelphati, O.; Szoka, F. C. *Proc. Natl. Acad. Sci. U.S.A.* **1996**, *93*, 11493–11498.

may occur within the endosomes, where an even higher local glycosaminoglycan concentration is presented to the polyplexes. Moreover, if the polymer is able to buffer the acidification event that occurs in the endosomes (which is believed to signal fusion with the lysosomes and activate degradative enzymes), some of the pDNA may not be degraded by delaying the lysosomal fusion event and thus remain intact.⁵⁸ Studies are currently ongoing to further examine these phenomena which are important to give us insight into the chemical properties that produce the most efficient and nontoxic nucleic acid delivery. Advancing the knowledge of how the polymer chemistry affects the biological processes involved in the cellular transport of

(58) Erbacher, P.; Roche, A. C.; Monsigny, M.; Midoux, P. *Exp. Cell Res.* **1996**, *225*, 186–194.

nucleic acids is essential to the future rational design of synthetic vectors and will facilitate the use of nucleic acid drugs in many revolutionary medical treatments.

Acknowledgment. The authors gratefully acknowledge funding of this work by the National Institutes of Health (1-R21-EB003938-01), the University of Cincinnati Research Council, the UC Department of Chemistry, and the UC Chemical Sensors Group. In addition, we thank Dr. Matt Lynch, Procter and Gamble Inc., for generous use of the dynamic light scattering instrument and Laura Wenning for performing some of the gel shift assays. Y.L. thanks the University of Cincinnati for the Chemical Sensors and Laws-Stecker graduate fellowships.

JA0436446